PHYSICAL REVIEW E **66**, 020802(R) (2002)

Permeability and conductivity of platelet-reinforced membranes and composites

T. F. Nagy* and P. M. Duxbury
Department of Physics/Astronomy and Center for Fundamental Materials Research, Michigan State University, East Lansing, Michigan 48824

(Received 10 April 2002; published 13 August 2002)

We present large-scale simulations of the diffusion constant D of a random composite consisting of aligned platelets with aspect ratio $a/b \gg 1$ in a matrix (with diffusion constant D_0) and find that $D/D_0 = 1/(1 + c_1 x + c_2 x^2)$, where $x = a v_f / b$ and v_f is the platelet volume fraction. We demonstrate that for large aspect ratio platelets the pair term (x^2) *dominates* suggesting large property enhancements for these materials. However, a small amount of face-to-face ordering of the platelets *markedly degrades* the efficiency of platelet reinforcement.

DOI: 10.1103/PhysRevE.66.020802 PACS number(s): 81.05.Qk, 66.30.Pa, 87.53.Wz

Thin reinforcing platelets can be extremely effective at improving the barrier and in-plane mechanical properties of composites and membranes. In particular there has been an explosion of interest in clay-reinforced thermoplastics, thermosets, and rubbers, with target applications ranging from packaging to cars [1–5]. To achieve the theoretically promised enhancements requires well-aligned and well-dispersed clay platelets in these polymer matrices.

The traditional theory of composite reinforcement is based on single-inclusion theories that form a basis for self-consistent or effective-medium approximations. However, the effect of aligned reinforcing platelets is *not* correctly described by single-inclusion models, except at very low inclusion concentrations, even though many publications assume this approximation [6,7]. The correct variable to use in describing platelet reinforcement in the large aspect ratio limit is the product of the aspect ratio (a/b) *times* the volume fraction (v_f), $x = a v_f / b$. Since the aspect ratio of clay platelets ranges from 100–2000, x is typically not small as even a 1% inclusion volume fraction leads to large values of x. We calculate the diffusion constant in regimes where x is not small [8,9] and derive a simple form that represents the data well. We find that the *quadratic term* dominates (i.e., a term proportional to x^2) and its dominance is due to the narrow necks between platelets that are not included in single-inclusion theories.

However, chemically nanodispersed clay platelets tend to order themselves face-to-face into stacks as seen in Fig. 3. In a thermodynamic picture this corresponds to a phase separation of the material into platelet rich and platelet poor regions. In the platelet poor regions the diffusion is relatively easy. We calculate the dependence of the diffusion constant on face-to-face alignment and show that the rule of mixtures works effectively. In clay-polymer materials deleterious platelet-poor regions are broken up by using extrusion or mechanical mixing. To date no one has found a way to chemically modify the clays so that they prefer to arrange themselves in a more optimal (e.g., staggered) array. Nevertheless, theoretical studies suggest that nematic and staggered phases can be thermodynamically stable [10].

*Email address: nagy_t@pa.msu.edu

The leading-order term in the reduction in permeability due to platelet reinforcement is familiar in the composites community, though in a different context. There it is well known that a number density of aligned cracks, $n = N/V$ (N is the number of cracks and V is the sample volume), reduces the conductivity of a material of initial conductivity σ_0 according to

$$\sigma = \sigma_0 (1 - \pi a^2 n + \cdots) \tag{1}$$

for slits of length $2a$ in a homogeneous two-dimensional medium [11], and

$$\sigma = \sigma_0 \left(1 - \frac{8}{3} a^3 n + \cdots \right) \tag{2}$$

for penny-shaped cracks of radius a in a homogeneous three-dimensional medium [12]. The perpendicular (i.e., normal to the crack surface) conductivity of cracked solids σ/σ_0, the perpendicular permeability, k/k_0, of platelet-reinforced membranes and the perpendicular diffusion constant measured in platelet-reinforced membranes, D/D_0, are related by $\sigma/\sigma_0 = k/k_0 = D(1 - v_f)/D_0$. However, the experimental results for the permeability of barrier films are presented as a function of inclusion volume fraction v_f. This is derived simply from Eqs. (1) and (2) by using $v_f = n v^*$, where v^* is the volume of an inclusion. Thus for barrier membranes, the leading-order behavior for aligned rectangular sticks in two dimensions ($v^* = 4ab$) is

$$\frac{k}{k_0} = 1 - \frac{\pi}{4} \frac{a v_f}{b} + \cdots, \tag{3}$$

and for aligned penny-shaped platelets of radius a and thickness $2b$ is,

$$\frac{k}{k_0} = 1 - \frac{4}{3\pi} \frac{a v_f}{b} + \cdots. \tag{4}$$

The importance of the variable $x = a v_f / b$ is evident from these expresssions. In the barrier film community the reduction in permeability due to platelets is approximated in a different way [6,7]. There it is argued that for high aspect ratio platelets, the increased tortuousity of typical diffusion

paths L_p/L_0 gives the qualitatively correct reduction in the diffusion constant, i.e., $D/D_0 \sim L_0/L_p$. The dependence of path tortuousity on inclusion volume fraction is given by $L_p/L_0=(1+av_f/2b)$, where a/b is the platelet aspect ratio. Note that this is of the same form as an effective-medium theory based on Eqs. (3) and (4). However, as we now show, this tortuousity argument is *qualitatively incorrect* for platelet-reinforced materials and if done correctly leads to a quadratic [i.e., $O(b/(av_f))^2$] reduction in the diffusivity in both two and three dimensions.

We use the resistor respresentation to calculate the effect of tortuous diffusion paths on the overall conductivity, permeability, and diffusivity. Consider a composite composed of randomly centered, aligned, nonoverlapping, insulating sticks or pennies placed in a matrix of conductivity σ_0. We define the typical perpendicular distance between inclusions to be l. The volume fraction is related to l via, $v_f \approx 2b/(l+2b) \approx 2b/l$ as the inclusion volume fractions that are observed for high aspect ratio materials are typically less than 10%. A tortuous path through a random array of these aligned platelets is approximated by a series combination of resistors each of which has the typical resistance

$$r_t \approx \frac{\rho_0 a}{l a^{d-2}}, \tag{5}$$

where $\rho_0=1/\sigma_0$. This resistance is calculated by considering a "neck" of matrix material between two adjacent inclusions. This resistor has a typical length of order a (we drop constant prefactors) and cross section of order la^{d-2}. In a film of thickness t, the resistance of a tortuous path is then $R_t=r_t(t/(l+2b)) \approx \rho_0 t a^{3-d}/l^2$. In a composite of transverse dimension L_t (perpendicular to the thickness direction), however, there are many parallel paths of this sort and their conductances must be added to approximate the overall permeability or conductivity. The typical number of such paths is $(L_t/a)^{d-1}$, so that the typical resistance of a composite of dimensions $L_t^{d-1}t$ is $R_f \approx \rho_0 t a^{3-d}/(L_t/a)^{d-1} l^2$. We are interested in the conductivity ($\propto$ permeability) which is related to the resistance by $\sigma=t/R_f(L_t)^{d-1}$. Using $v_f=b/l$, we thus find

$$\sigma \approx \sigma_0 \left(\frac{b}{a v_f}\right)^2 = \sigma_0 \frac{1}{x^2}. \tag{6}$$

This result is due to the necks between platelets and is thus a pair term and is not included in single-inclusion theories. Note that if the matrix conductivity was dependent on the neck width, as might occur if there was enhanced trapping of diffusants in the necks, their effect could be easily incorporated in the sum of effective resistors along a typical path. In order to find a typical value for the prefactor of the quadratic term, and to compare its importance with the linear term found from single-inclusion theories [Eq. (3) and (4)], we have carried out large-scale simulations. To compare the above theory with the simulations, we need to include both the leading-order term [Eq. (3) and (4)] and the quadratic term (6) in our analysis. The simplest form that contains both of these terms is

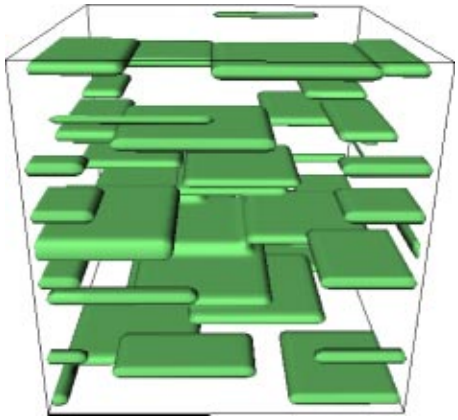

FIG. 1. Aligned square platelets randomly embedded in a three-dimensional cube. The aspect ratio $a/b=25$, the boundary conditions are periodic in all directions.

$$\frac{D}{D_0} = \frac{1}{1+c_1 x + c_2 x^2}, \tag{7}$$

where $x=av_f/b$. As we show below, this form works extremely well for aligned non-overlapping, well-dispersed platelets over a broad range of concentrations. Important corrections occur if the platelets stick to each other or if the platelets overlap (i.e., percolation effects) and we shall present the details of these effects elsewhere.

Our calculation of the effective diffusivity of clay-reinforced membranes is carried out as follows. Clay platelets act as effective diffusion barriers to molecules such as oxygen and water, so we assign them diffusion constant zero. In contrast, many polymers are oxygen and water permeable so we assign the matrix a finite diffusion constant D_0. We calculate the effective diffusion constant of a polymer containing volume fraction v_f of aligned platelets, as illustrated in Fig. 1. The effective diffusion constant of these composites is found by embedding the geometry in large square or cubic lattices. Random walkers are then started at random locations in these geometries. The end-to-end distance of these walkers is monitored as a function of time. Averaging the trajectories leads to the average diffusive behavior $\langle r^2 \rangle \propto Dt$. The effective diffusion constant is then found by extracting the slope of a plot of $\langle r^2 \rangle$ versus t. Our code for the "blind ant" [13] method described above is very efficient, which enables simulations on very large lattices over long times. This is essential for the large aspect ratio composites discussed here. Note that $k/k_0=D(1-v_f)/D_0$ due to the fact that random walkers cannot be placed on the zero permeability barriers. In experiments, the permeability is measured by placing the barrier in a pressure gradient, with pressure p of gas (e.g., Oxygen) on one side of the membrane and the other side maintained at a very low pressure. The steady-state flux of gas, f, through the membrane is measured and

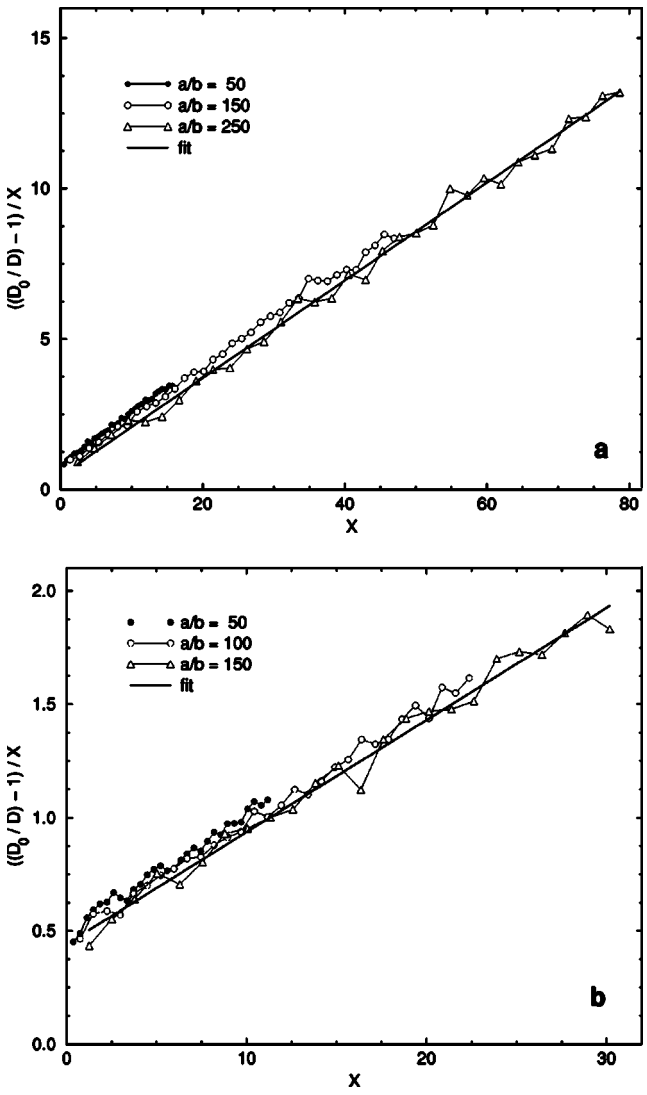

FIG. 2. Tests of the form (7) of the text. A plot of $(D_0/D-1)/x$ as a function of $x=av_f/b$, where a/b is the platelet aspect ratio and v_f their volume fraction. The solid lines are fits to the largest aspect ratio data. (a) Data for aligned slits randomly placed, without overlap, onto a square lattice. The simulations were carried out on square lattices of size 2048^2, over 6×10^4 steps in the blind ant algorithm (see text) and averaged over 30 000 configurations. (b) Data for aligned squares (see Fig. 1) placed, without overlap, onto a cubic lattice. The simulations were carried out on cubic lattices of size 512^3, over 5×10^4 steps in the blind ant algorithm (see text) and averaged over 20 000 configurations.

the permeability $k=p/f$. The diffusion constant is measured by tracking the tracer diffusion of tagged particles, for example, using NMR.

A high-precision test of Eq. (7) is presented in Fig. 2(a) for the sticks aligned in two dimensions and Fig. 2(b) for the squares aligned in three dimensions. We plot the quantity $(D_0/D-1)/x$ which, if Eq. (7) is correct, should be linear, i.e., $(D_0/D-1)/x=c_1+c_2x$. The data of Fig. 2 confirms this form remarkably well over the entire range of inclusion concentrations, even close to the dense packing limit. A linear fit to the data of Fig. 2 yields the coefficients to the

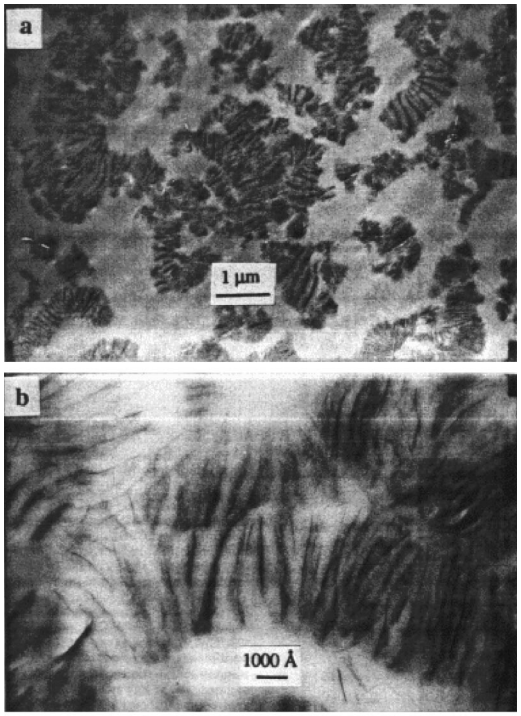

FIG. 3. Experimental platelet morphology at two length scales. (a) The upper figure shows that there is a phase separation into platelet rich and platelet poor regions. (b) The lower figure illustrates the face-to-face alignment of the platelets. The dark regions are clay, the light regions are the polymer (from Ref. [14]).

quadratic term, $c_2^{2d}=0.165\pm0.01$ [from Fig. 2(a)], and $c_2^{3d}=0.050\pm0.005$ [from Fig. 2(b)]. The leading-order coefficient in the concentration expansion c_1 is quite poorly converged in two dimensions. From Fig. 2(a), it is seen that this c_1^{2d} is still decreasing even for large aspect ratio platelets. For the largest aspect ratios we studied its value is $c_1^{2d}(a/b=250)=0.46\pm0.01$. In three dimensions the convergence is much better and we find $c_1^{3d}=0.44\pm0.03$. The theoretical values [from Eqs. (3) and (4)] are $c_1^{slit}=\pi/4=0.785\ldots$, and $c_1^{penny}=4/(3\pi)=0.425\ldots$, respectively. The numerical simulations are on lattices and so cannot be expected to be exactly the same as the continuum results (3) and (4). Nevertheless, it is clear that materials reinforced by well-dispersed platelets are *not* correctly described by effective-medium theory based on a linear expansion in x, or the Nielsen formula $[D/D_0=1/(1+x/2)]$ which is used in the diffusion community [6,7]. An important consequence of this result is that the property enhancements that are theoretically possible from platelet-reinforced materials, for example, clay-polymer nanocomposites, are *much larger* than has previously been suggested or observed.

The real morphology of, as synthesized, clay-polymer materials is illustrated in Fig. 3 [14]. The strong face-to-face packing of the platelets and the presence of large platelet-free regions of the matrix material is evident. These materials do not provide the barrier performance promised by the result Eq. (7). The platelet-free regions of the matrix material form channels at a larger length-scale and act as a diffusion ''short-circuit'' so that the effective diffusion constant of the

composite remains closer to that of the pure matrix material. In order to make the diffusion paths through the matrix material more tortuous, materials such as this are mixed in extruders or sheared in other ways in order to produce better platelet dispersion. A simple model for various degrees of platelet phase separation on the diffusion constant is illustrated in Fig. 4. The platelets are initially in a perfectly staggered array and then one sublattice of the array is shifted by an amount $0 \leqslant s \leqslant a$ until the platelets are in a perfect face-to-face arrangement. Clearly, even a small amount of phase separation (finite s) yields higher permeability. In fact a careful study of this effect indicates that if the reduction in diffusion constant promised by the formula (6) is 1000-fold, matrix channels of size 1/1000 or larger will be deleterious for the composite performance. This means that platelet dispersion must be very good indeed to achieve the full performance enhancements promised by large aspect ratio platelets. Note that if there was a distribution of channel sizes and a distribution of platelet sizes, as would occur in most real materials, their effect is well approximated by treating the channels as a parallel set of resistors.

In summary, we have shown that the effective diffusion constant (as well as the conductivity and permeability) of platelet-reinforced composites is not well described by single-inclusion theories, even though almost all experimental studies in the literature use expressions that are based on this limit. This is good news, as it means that the theoretically possible property enhancements are *quadratic* in the volume fraction, rather than linear. This general result should also apply to many other transport and mechanical properties of well-dispersed platelet reinforced materials, and is due to the dominance of narrow necks in large aspect ratio limit. However, we also showed that face-to-face platelet ordering is extremely deleterious to the performance of these materials (see Fig. 4), so that achieving the full enhancements promised by these materials remains a challenging synthesis problem.

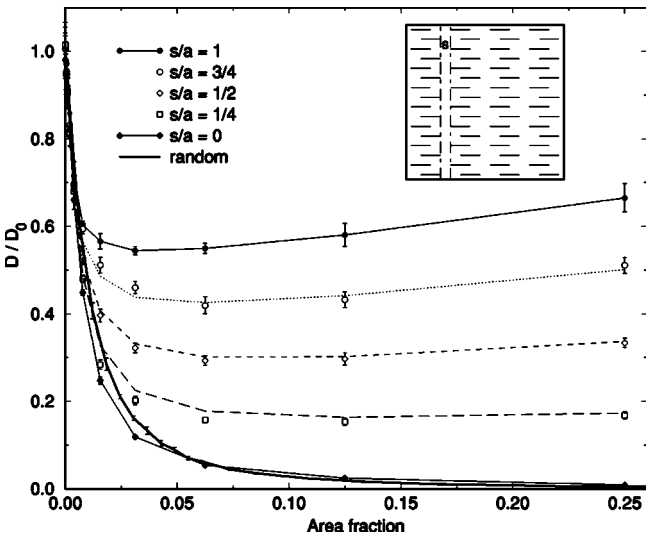

FIG. 4. The effective diffusion constant as a function of face-to-face alignment of the platelets. The inset shows one of the geometries that was used for the calculations. The aspect ratio a/b is fixed at the value of 128. The ratio s/a changes from 0 to 1 using a stepsize of 1/4. $s/a=0$ corresponds to the staggered arrangement of the platelets, while $s/a=1$ corresponds to the configuration consisting of straight columns of face-to-face ordered platelets and straight platelet-free channels. The width of the matrix channel is s. The inset shows the configuration for $s/a=1/2$. Also included are the data for a random system with the same aspect ratio and they show that the random system is not significantly different from the perfectly staggered array of barriers. The three plots at intermediate s/a (dots, small dashes, and large dashes) are interpolations between the $s/a=0$ and $s/a=1$ values using the rule of mixtures.

This work has been supported by the DOE under Contract No. DE-FG02-90ER45418 through a supplement from the CMSN program, by a grant from Ford research and by the composite materials and structures center at MSU.

[1] Y. Kojima, A. Usuki, M. Kawasumi, A. Okada, T. Kurauchi, and O. Kamigaito, J. Polym. Sci. A **31**, 983 (1993).

[2] P. Lan, P.D. Kaviratna, and T.J. Pinnavaia, Chem. Mater. **7**, 2144 (1995).

[3] E.P. Giannelis, R. Krishnamoorti and E. Manias, Adv. Polym. Sci. **138**, 107 (1999).

[4] L.M. Sherman, Plast. Technol. **45**(6), 52 (1999).

[5] J.M. Garces, D.J. Moll, J. Bicerano, R. Fibiger, and D.G. McLeod, Adv. Mater. **12**, 1835 (2000).

[6] K. Yano, A. Usuki, A. Okada, T. Kurauchi, and O. Kamigaito, J. Polym. Sci. A **31**, 2493 (1993).

[7] L.E. Nielsen, J. Macromol. Sci., Chem. **A1**, 929 (1967); D.J. Sekelik, E.V. Stepanov, S. Nazarenko, D. Schiraldi, A. Hiltner, and E. Baer, J. Polym. Sci., Part B: Polym. Phys. **37**, 847 (1999).

[8] E.L. Cussler, S.E. Hughes, W.J. Ward III, and R. Aris, J. Membr. Sci. **38**, 161 (1988); W.R. Falla, M. Mulski and E.L. Cussler, *ibid.* **119**, 129 (1996).

[9] G.H. Fredrickson and J. Bicerano, J. Chem. Phys. **110**, 2181 (1999).

[10] V.V. Ginzburg, C. Singh, and A.C. Balazs, Macromolecules **33**, 1089 (2000).

[11] For a recent discussion, see M.F. Thorpe, Proc. R. Soc. London, Ser. A **437**, 215 (1992), Eq. (43).

[12] For a recent discussion, see B. Shafiro and M. Kachanov, J. Appl. Phys. **87**, 8561 (2000), Eq. (9).

[13] L. Puech and R. Rammal, J. Phys. C **35**, L1197 (1983); J. Tobochnik, D. Laing, and G. Wilson, Phys. Rev. A **41**, 3052 (1990); I.C. Kim and S. Torquato, J. Appl. Phys. **74**, 1844 (1993).

[14] M.S. Wang and T.J. Pinnavaia, Chem. Mater. **6**, 468 (1994).